

# Solar Extreme UV radiation and quark nugget dark matter model

**Ariel Zhitnitsky**

Department of Physics & Astronomy, University of British Columbia, Vancouver, B.C. V6T 1Z1, Canada

**Abstract.** We advocate the idea that the surprising emission of extreme ultra violet (EUV) radiation and soft x-rays from the Sun are powered externally by incident dark matter (DM) particles. The energy and the spectral shape of this otherwise unexpected solar irradiation is estimated within the quark nugget dark matter model. This model was originally invented as a natural explanation of the observed ratio  $\Omega_{\text{dark}} \sim \Omega_{\text{visible}}$  when the DM and visible matter densities assume the same order of magnitude values. This generic consequence of the model is a result of the common origin of both types of matter which are formed during the same QCD transition and both proportional to the same fundamental dimensional parameter  $\Lambda_{\text{QCD}}$ .

We also present arguments suggesting that the transient brightening-like “nanoflares” in the Sun may be related to the annihilation events which inevitably occur in the solar atmosphere within this dark matter scenario.

---

## Contents

<b>1</b>	<b>Introduction</b>	<b>1</b>
<b>2</b>	<b>Axion Quark Nugget (AQN) dark matter model</b>	<b>4</b>
<b>3</b>	<b>Anti-nuggets in the Sun</b>	<b>7</b>
3.1	The Basic Features of the Spectrum	8
3.2	The annihilation pattern. The big picture.	10
<b>4</b>	<b>Observation of nanoflares as evidence for anti-nuggets in Corona</b>	<b>12</b>
4.1	Few historical remarks on nanoflares	12
4.2	Nanoflares as the annihilation events of the anti-nuggets	13
4.3	Recent advances and Future development	14
<b>5</b>	<b>Sun as an ideal place to study AQN dark matter model</b>	<b>17</b>
<b>6</b>	<b>Concluding remarks and Wild speculations.</b>	<b>18</b>
<b>A</b>	<b>Few technical characteristics of the anti-nuggets at <math>T \neq 0</math></b>	<b>20</b>

---

## 1 Introduction

A variety of anomalous solar phenomena still defy conventional theoretical understanding. For example, the detailed physical processes that heat the outer atmosphere of the Sun to  $10^6\text{K}$  remain a major open issue in astrophysics [1]. In the past, numerous theoretical models have been persuaded, but they failed to provide a quantitative explanation. We mention a few ideas related, e.g., to neutrons, interplanetary matter, acoustic waves and gravity waves [1–4]. Therefore, after several decades of research, it may be that the answer lies in new physics. A first suggestion was made in 2002 [5], assuming gravitationally trapped or radiatively decaying massive axion-like particles being produced in the hot solar core. The main goal of the present work is to formulate a new proposal which may potentially resolve the old renowned puzzle (since 1939) known in the community under the name “the Solar Corona Mystery”. This persisting puzzle is characterized by the following observed anomalous behaviour of the sun [5],[6]:

- The quiet Sun emits an extreme ultra violet (EUV) radiation with a photon energy of order of hundreds of eV which cannot be explained in terms of any conventional astrophysical phenomena;
- The total energy output of the corona is about  $(10^{-7} - 10^{-6})$  times that of the photosphere ( $L_{\text{corona}} \sim 10^{27}$  erg/s ), which never drops to zero as time evolves. So far, no viable conventional mechanism(s) could explain this far beyond thermal equilibrium emission of radiation;
- Spatially, the unexpected EUV emission occurs near the transition region (TR), about 2000 km above the solar surface, see Fig. 1. At first sight, it could be interpreted as the emission from a hot gas with the temperature  $T \simeq 3 \cdot 10^5$  K. Though, how the

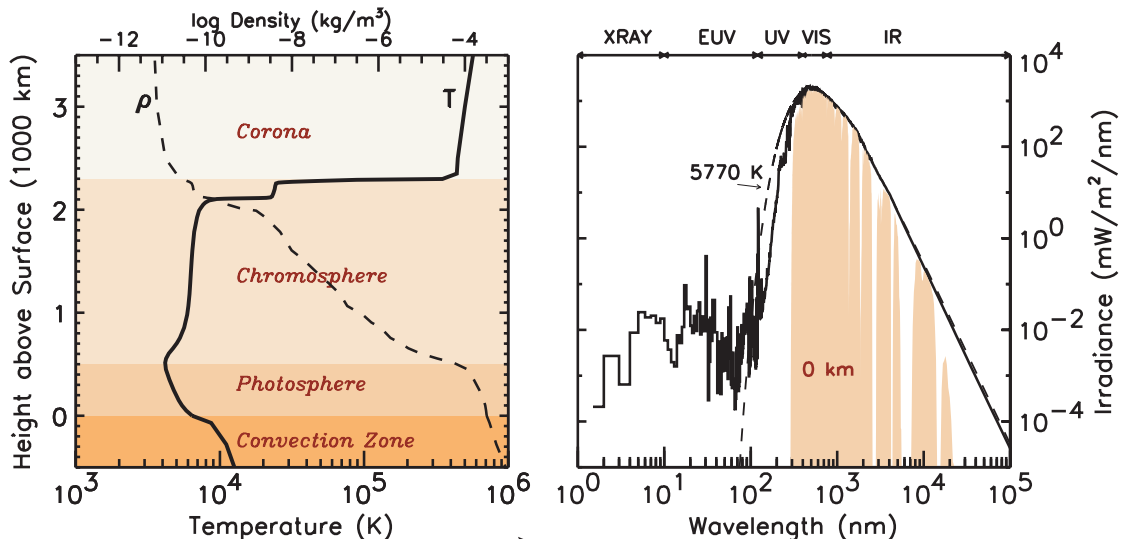


**Figure 1.** Left: The temperature distribution of the inner and outer Sun. The drastic changes occur in vicinity of 2000km. Right: the unexpected deviation from the thermal distribution in the extreme ultraviolet (EUV) and soft x-rays in the solar spectrum constitutes the celebrated solar corona problem. This EUV and x-ray radiation is originated from chromosphere, transition and corona regions. The total EUV intensity represents a small  $\sim (10^{-7} - 10^{-6})$  portion of the solar irradiance. The plots are taken from [5].

underlying gas heating takes place is a long lasting question for solar physics. The TR is the most spectacular place in the Sun, since it is where the mysterious temperature inversion appears;

- At the transition region, the (quiet Sun) temperature continues to rise very steeply until it reaches a few  $10^6$  K, i.e., being a few 100 times hotter above the underlying photosphere, and this within an atmospheric layer thickness of only 100 km or even much less, see Fig. 1. One should keep in mind that the density at the place where this step occurs is about  $10^{-(12\pm 1)}$  g/cm<sup>3</sup>, i.e. an excellent vacuum, which actually does not facilitate a conventional explanation of this observation.

Following conventional physics, it is fair to say that *everything above the photosphere is not supposed to be there at all*. Therefore, the corona / chromosphere heating problem cannot be solved without invoking energization processes.

Qualitatively, this peculiar behaviour of the Sun atmosphere is suggesting for some external irradiation (pressure) acting continuously on the whole Sun. Interestingly, also transient heating events of active regions (AR), including the concepts of “micro-events”, “micro-flares” and “nanoflares” [7], have been previously considered to be of potential interest for understanding the coronal heating mechanism [8] because they may give rise to a basal background heating near the solar surface.

In the present work we advocate a drastically different scenario when the energy deposition is originated from outside the system, in contrast with previously considered proposals when the energy is originated from the deep dense regions of the sun. We want to argue that the observed peculiar behaviour might be intimately related to this fundamentally distinct scenario when the extra source of the energy is associated with the dark matter nuggets continuously entering the sun from outer space. A large amount of energy is available in our proposal as result of huge energy deposition of such dark matter constituents (represented in the model [9] by the quark nuggets made of matter and *antimatter*) before being disintegrated as described below.

In fact, our proposal is largely motivated by the following numerical observation. It has been known for quite some time that the total intensity of the observed EUV and soft x-ray radiation (averaged over time) can be estimated as follows,

$$L_{\odot} \text{ (from Corona)} \sim 10^{30} \cdot \frac{\text{GeV}}{\text{s}} \sim 10^{27} \cdot \frac{\text{erg}}{\text{s}}. \quad (1.1)$$

The corresponding flux from solar corona measured on the Earth is estimated as

$$\Phi_{\oplus} \text{ (from Corona)} \sim 10^3 \cdot \frac{\text{GeV}}{\text{cm}^2 \cdot \text{s}} \sim 10^{-7} \cdot \frac{\text{W}}{\text{cm}^2}, \quad (1.2)$$

which represents about  $(10^{-7} - 10^{-6})$  fraction of the solar luminosity. It turns out that if one estimates the extra energy being produced within the dark matter scenario (originally suggested in [9] for completely different purposes) one obtains the total extra energy  $\sim 10^{27} \text{erg/s}$  which precisely reproduces (1.1) for the observed EUV and soft x-ray intensities. One should add that the estimate  $\sim 10^{27} \text{erg/s}$  for extra energy is derived exclusively in terms of known dark matter density  $\rho_{\text{DM}} \sim 0.3 \text{ GeVcm}^{-3}$  and dark matter velocity  $v_{\text{DM}} \sim 10^{-3}c$  surrounding the sun without adjusting any parameters of the model, see section 3 below with relevant estimates. We interpret this “numerical coincidence” as an additional hint supporting our, naively “very speculative” (but in our view very sound) proposal.

We shall argue below that the unusual features of the solar EUV and soft x-rays, being emitted continuously and / or burst-like, can be naturally explained by the quark nugget dark matter model which was originally formulated in [9] for completely different purposes. To be more specific, this model was invented as a natural explanation of the observed ratio  $\Omega_{\text{dark}} \sim \Omega_{\text{visible}}$ . The similarity between dark matter  $\Omega_{\text{dark}}$  and the visible matter  $\Omega_{\text{visible}}$  densities strongly suggests that both types of matter have been formed during the same cosmological epoch, which must be the QCD transition as the baryon mass  $m_p$  which represents the visible portion of the matter  $\Omega_{\text{visible}}$  is obviously proportional to  $\Lambda_{\text{QCD}}$ , while the contribution related to the Higgs physics represents only a minor contribution to the proton mass.

Before turning to the details of the EUV emission from the sun within this framework we will first give a brief overview of the quark nugget dark matter model in Section 2. In Section 3 we argue that the total energy deposition within this model is of order  $(10^{-7} - 10^{-6})$  times that of the photosphere, which is precisely the observed ratio (1.1) as mentioned above.

Furthermore, we also estimate the spectrum of the radiation due to this mechanism. We find it is consistent with observations corresponding to the plasma temperature  $T \simeq 10^6\text{K}$ . In Section 4 we make one step further and present few arguments suggesting that the observed “nanoflares” in quiet regions can be identified with annihilation events of the anti-nuggets in our framework as they fit features observed by SoHO/EIT instrument<sup>1</sup>. In Section 5 we explain the drastic differences between the collisions of the nuggets with Earth and the Sun, suggesting that the Sun is an ideal system to test this dark matter model. In concluding section 6 we make few speculative comments on possible relations of our framework with other mysterious and puzzling phenomena which are observed, but not understood yet.

## 2 Axion Quark Nugget (AQN) dark matter model

The idea that the dark matter may take the form of composite objects of standard model quarks in a novel phase goes back to quark nuggets [10], strangelets [11], nuclearities [12], see also review [13] with large number of references on the original results. In the models [10–13] the presence of strange quark stabilizes the quark matter at sufficiently high densities allowing strangelets being formed in the early universe to remain stable over cosmological timescales. There were a number of problems with the original idea<sup>2</sup> and we refer to the review paper [13] for the details.

The AQN model in the title of this section stands for the axion quark nugget model [9] to emphasize on essential role of the axion field in the construction and to avoid confusion with earlier models [10–13] mentioned above. The AQN model suggested in [9] is drastically different from previous proposals in two key aspects:

1. There is an additional stabilization factor in the AQN model provided by the axion domain walls which are copiously produced during the QCD transition<sup>3</sup>.
2. The AQN could be made of matter as well as *antimatter* in this framework as a result of separation of charges, see original papers [9, 16, 17] and short review [18].

The most important astrophysical implication of these new aspects relevant for the present studies of the EUV radiation is that quark nuggets made of antimatter store a huge amount of energy which can be released when the anti-nuggets hit the solar surface and get annihilated. This feature of the AQN model is unique and is not shared by any other dark matter models because the dark matter in AQN model is made of the same quarks and antiquarks of the standard model (SM). One should also remark here that the annihilation events of the anti-nuggets with visible matter may produce a number of other observable effects in different circumstances such as rare events of annihilation of anti-nuggets with

---

<sup>1</sup>We want to avoid any confusions with the terminology and refer to “nanoflares” as the “micro-events” in *quiet* regions of corona to be contrasted with “micro-flares” which are significantly larger in scale and observed almost exclusively in *active* regions, see section 4 for the precise definitions adopted in the present work.

<sup>2</sup>In particular, the first order phase transition is a required feature of the system for the strangelet to be formed during the QCD phase transition. However it is known by now that the QCD transition is a crossover rather than the first order phase transition as the recent lattice results [14] unambiguously show. Furthermore, the strangelets will likely evaporate on the Hubble time-scale even if they had been formed [15].

<sup>3</sup>The direct consequence of this additional element is that the first order phase transition is not required for the nuggets to be formed as the axion domain wall plays the role of the squeezer. Furthermore, the argument related to the fast evaporation of the strangelets as mentioned in footnote 2 is not applicable for the AQN model [9] because the vacuum ground state energies inside and outside the nuggets are drastically different. Therefore these two systems can coexist only in the presence of the additional external pressure provided by the axion domain wall.

visible matter in the centre of galaxy, or in the Earth atmosphere, see some comments and references at the end of this section.

The basic idea of the proposal [9] can be explained as follows: It is commonly assumed that the universe began in a symmetric state with zero global baryonic charge and later (through some baryon number violating process, the so-called baryogenesis) evolved into a state with a net positive baryon number. As an alternative to this scenario we advocate a model in which “baryogenesis” is actually a charge separation process in which the global baryon number of the universe remains zero. In this model the unobserved antibaryons come to comprise the dark matter in the form of dense nuggets of quarks and antiquarks in colour superconducting (CS) phase. The formation of the nuggets made of matter and antimatter occurs through the dynamics of shrinking axion domain walls, see original papers [19, 20] with the details.

The nuggets, after they formed, can be viewed as the strongly interacting and macroscopically large objects with a typical nuclear density and with a typical size  $R \sim (10^{-5} - 10^{-4})$  cm determined by the axion mass  $m_a$  as these two parameters are linked,  $R \sim m_a^{-1}$ . This relation between the size of nugget  $R$  and the axion mass  $m_a$  is a result of the equilibration between the axion domain wall pressure and the Fermi pressure of the dense quark matter in CS phase. One can easily estimate a typical baryon charge  $B$  of such macroscopically large objects as the typical density of matter in CS phase is only few times the nuclear density. Therefore, a typical baryon charge of a nugget ranges from  $B \sim 10^{24}$  to  $B \sim 10^{28}$ , depending on the mass of the axion, yet to be discovered. The corresponding mass  $M$  of the nuggets can be estimated as  $M \sim m_p B$ , where  $m_p$  is the proton mass.

This model is perfectly consistent with all known astrophysical, cosmological, satellite and ground based constraints within the parametrical range mentioned above. It is also consistent with known constraints from the axion search experiments. Furthermore, there is a number of frequency bands where some excess of emission was observed, but not explained by conventional astrophysical sources. Our comment here is that this model may explain some portion, or even entire excess of the observed radiation in these frequency bands, see short review [18] and additional references at the end of this section.

Another key element of this model is the coherent axion field  $\theta$  which is assumed to be non-zero during the QCD transition in early Universe. If the fundamental  $\theta$  parameter of QCD were identically zero during the formation time, equal numbers of nuggets made of matter and antimatter would be formed. However, the fundamental  $\mathcal{CP}$  violating processes associated with the  $\theta$  term in QCD result in the preferential formation of antinuggets over nuggets<sup>4</sup>. This source of strong  $\mathcal{CP}$  violation is no longer available at the present epoch as a result of the axion dynamics when  $\theta$  eventually relaxes to zero, see original papers [21–23] and recent reviews [24–31] on the axion dynamics and recent searches of the axions.

As a result of these  $\mathcal{CP}$  violating processes the number of nuggets and anti-nuggets being formed would be different. This difference is always of order of one effect [19, 20] irrespectively to the parameters of the theory, the axion mass  $m_a$  or the initial misalignment angle  $\theta_0$ . As a result of this disparity between nuggets and anti nuggets a similar disparity would also emerge between visible quarks and antiquarks.

This disparity implies that the total number of antibaryons will be less than the number of baryons in early universe plasma. These anti-baryons will be soon annihilated away leaving only the baryons whose antimatter counterparts are bound in the excess of antiquark nuggets

---

<sup>4</sup>This preference is essentially determined by the sign of initial  $\theta_0$  before it relaxes to zero due to the axion dynamics.

and are thus unavailable to annihilate. All asymmetries are of order of one effects. This is precisely the reason why the resulting visible and dark matter densities must be the same order of magnitude [19, 20]

$$\Omega_{\text{dark}} \sim \Omega_{\text{visible}} \quad (2.1)$$

as they are both proportional to the same fundamental  $\Lambda_{\text{QCD}}$  scale, and they both are originated at the same QCD epoch. If these processes are not fundamentally related the two components  $\Omega_{\text{dark}}$  and  $\Omega_{\text{visible}}$  could easily exist at vastly different scales.

Another fundamental ratio (along with  $\Omega_{\text{dark}} \sim \Omega_{\text{visible}}$  discussed above) is the baryon to entropy ratio at present time

$$\eta \equiv \frac{n_B - n_{\bar{B}}}{n_\gamma} \simeq \frac{n_B}{n_\gamma} \sim 10^{-10}. \quad (2.2)$$

In our proposal (in contrast with conventional baryogenesis frameworks) this ratio is determined by the formation temperature  $T_{\text{form}} \simeq 41$  MeV at which the nuggets and antinuggets compete their formation, when all anti baryons get annihilated and only the baryons remain in the system, see details in [19]. We note that  $T_{\text{form}} \approx \Lambda_{\text{QCD}}$ . This temperature is determined by the observed ratio (2.2). The  $T_{\text{form}}$  assumes a typical QCD value, as it should as there are no any small parameters in QCD.

One can recapitulate the same claim in terms of the cosmological time  $t$  instead of the temperature  $T$ . As it is known the QCD transition happens at  $T \simeq 170$  MeV which corresponds to cosmic time  $t_0 \simeq 10^{-4}$  s. During the radiation epoch the temperature scales as  $T \sim t^{-1/2}$ . Therefore, the formation of the nuggets is completed around  $t_{\text{form}} \simeq 10^{-3}$  s which corresponds to the formation temperature  $T_{\text{form}} \simeq 41$  MeV when the baryon to entropy ratio assumes its present value (2.2).

Unlike conventional dark matter candidates, such as WIMPs (Weakly interacting Massive Particles) the dark-matter/antimatter nuggets are strongly interacting and macroscopically large as already mentioned. However, they do not contradict any of the many known observational constraints on dark matter or antimatter for three main reasons [17]:

- They carry very large baryon charge  $|B| \gtrsim 10^{24}$ , and so their number density is very small  $\sim B^{-1}$ . As a result of this unique feature, their interaction with visible matter is highly inefficient, and therefore, the nuggets are perfectly qualify as DM candidates. In particular, the quark nuggets essentially decouple from CMB photons, and therefore, they do not destroy conventional picture for the structure formation;
- The core of the nuggets have nuclear densities. Therefore, the relevant effective interaction is very small  $\sigma/M \sim 10^{-10}$  cm<sup>2</sup>/g. Numerically, it is comparable with conventional WIMPs values. Therefore, it is consistent with the typical astrophysical and cosmological constraints which are normally represented as  $\sigma/M < 1$  cm<sup>2</sup>/g;
- The quark nuggets have very large binding energy due to the large gap  $\Delta \sim 100$  MeV in CS phases. Therefore, the baryon charge is so strongly bounded in the core of the nugget that it is not available to participate in big bang nucleosynthesis (BBN) at  $T \approx 1$  MeV, long after the nuggets had been formed.

It should be noted that the galactic spectrum contains several excesses of diffuse emission the origin of which is unknown, the best known example being the strong galactic 511 keV



line. If the nuggets have the average baryon number in the  $\langle B \rangle \sim 10^{25}$  range they could offer a potential explanation for several of these diffuse components. It is important to emphasize that a comparison between emissions with drastically different frequencies in such a computations is possible because the rate of annihilation events (between visible matter and antimatter DM nuggets) is proportional to one and the same product of the local visible and DM distributions at the annihilation site. The observed fluxes for different emissions thus depend through one and the same line-of-sight integral

$$\Phi \sim R^2 \int d\Omega dl [n_{\text{visible}}(l) \cdot n_{DM}(l)], \quad (2.3)$$

where  $R \sim B^{1/3}$  is a typical size of the nugget which determines the effective cross section of interaction between DM and visible matter. As  $n_{DM} \sim B^{-1}$  the effective interaction is strongly suppressed  $\sim B^{-1/3}$ . The parameter  $\langle B \rangle \sim 10^{25}$  was fixed in this proposal by assuming that this mechanism saturates the observed 511 keV line [32, 33], which resulted from annihilation of the electrons from visible matter and positrons from anti-nuggets. Other emissions from different bands are expressed in terms of the same integral (2.3), and therefore, the relative intensities are unambiguously and completely determined by internal structure of the nuggets which is described by conventional nuclear physics and basic QED. In particular, the excess of the diffuse gamma ray emission in 1 – 20 MeV range observed by COMPTEL might be related with these annihilation processes of the galactic visible electrons with anti-nuggets, as argued in [34, 35]. For further details see the original works [32–38] and a short overview [18] with specific computations of diffuse galactic radiation in different frequency bands.

The studies which are most relevant for our present work is the analysis [39, 40] on neutrino emission from the Sun as a result of interaction of the antinuggets with solar environment. The basic claim of ref. [39] is as follows: if one assumes that the neutrino spectrum (as a result of annihilation of anti nuggets with matter in Sun) is similar to the spectrum observed in studies of low -energy  $p\bar{p}$  annihilation, then anti-quark nuggets cannot account for more than 1/5 of the dark matter flux.

This claim has been dismissed in ref. [40] by emphasizing that anti-nuggets cannot be treated as an usual antimatter in conventional hadronic phase as the quarks in nuggets (and antiquarks in anti nuggets) belong to CS phase rather than to the hadronic phase we are familiar with. In particular, the Nambu-Goldstone bosons in CS phase are 5-10 times lighter than their counterparts (such as conventional  $\pi$  mesons) in the hadronic phase. This observation leads to the profound consequences as the neutrino spectrum is expected to be in the 10 MeV range, in contrast with the 50 MeV scale associated with conventional hadronic decays as used in the analysis of [39]. Therefore, the quark nugget dark matter model is fully consistent with present neutrino flux measurements as stringent constraints from SuperK are not sensitive to the low energy neutrinos in the 10 MeV range [40].

### 3 Anti-nuggets in the Sun

We first present few basic relations from refs [39, 40] on the energy budget due to the capture of the anti-nuggets by the Sun. After that we focus on the spectral properties of the radiation from the anti nuggets when they interact with the matter from the Sun.

The impact parameter for capture of the nuggets by the Sun can be estimated as

$$b_{\text{cap}} \simeq R_{\odot} \sqrt{1 + \gamma_{\odot}}, \quad \gamma_{\odot} \equiv \frac{2GM_{\odot}}{R_{\odot}v^2}, \quad (3.1)$$



where  $v \simeq 10^{-3}c$  is a typical velocity of the nuggets. One can easily see that  $\gamma_{\odot} \gg 1$  which should be contrasted with the corresponding parameter on Earth,  $\gamma_{\oplus} \ll 1$ . Nuggets in the solar atmosphere will be decreasing their mass as result of annihilation, decreasing their kinetic energy and velocity as result of ionization and radiation.

Assuming that  $\rho_{\text{DM}} \sim 0.3 \text{ GeVcm}^{-3}$  and using the capture impact parameter (3.1), one can estimate the total energy flux due to the complete annihilation of the nuggets,

$$L_{\odot} (\text{AQN}) \sim 4\pi b_{\text{cap}}^2 \cdot v \cdot \rho_{\text{DM}} \simeq 3 \cdot 10^{30} \cdot \frac{\text{GeV}}{\text{s}} \simeq 4.8 \cdot 10^{27} \cdot \frac{\text{erg}}{\text{s}}, \quad (3.2)$$

where we substitute constant  $v \simeq 10^{-3}c$  to simplify numerical analysis. This estimate is very suggestive as it roughly coincides with the total EUV energy output (1.1) from corona which is hard to explain in terms of conventional astrophysical sources as highlighted in the Introduction. Precisely this ‘‘accidental numerical coincidence’’ was the main motivation to put forward the idea that (3.2) represents a new source of energy feeding the EUV radiation as advocated in this work. This source of the energy is unique to the AQN dark matter model as the energy is released as result of the annihilation of the antiquarks from anti nuggets with conventional baryonic matter in the solar Corona.

The corresponding flux due to the anti-nugget annihilations measured on the Earth is estimated as

$$\Phi_{\oplus} (\text{AQN}) \sim 10^3 \frac{\text{GeV}}{\text{cm}^2 \cdot \text{s}} \sim 1.6 \cdot 10^{-7} \frac{\text{W}}{\text{cm}^2}, \quad (3.3)$$

which should be compared with observed flux (1.2). The crucial observation of the present work is that while the total energy due to the annihilation of the anti-nuggets is indeed very small, nevertheless the anti-nuggets produce EUV spectrum characterized by the temperature  $T \sim 10^6\text{K}$  as explained below. Such spectrum observed in Corona is hard to explain by any conventional astrophysical processes as stated in the Introduction.

One should emphasize that the estimates (3.2) and (3.3) for the total intensity as well as the estimate for a typical temperature given in next subsection 3.1, are not sensitive to the size distribution of the nuggets. This is because the estimates (3.2) and (3.3) represent the total energy input due to the complete nugget’s annihilation, while their total baryon charge is determined by the dark matter flux  $\rho_{\text{DM}} \sim 0.3 \text{ GeVcm}^{-3}$ .

In contrast, there are many observables, to be mentioned in next sections 3.2 and 4 which are highly sensitive to the size distribution of the nuggets because the corresponding observables are expressed in terms of the baryon charge  $B$  of a nugget or its size  $R \sim B^{1/3}$ .

### 3.1 The Basic Features of the Spectrum

The goal here is to estimate the typical spectral properties of the radiation due to the annihilation of the anti-nuggets in solar environment. We follow ref. [36] in our estimation of the temperature of the anti-nuggets as they just enter the solar Corona.

The basic idea is to equate the total surface emissivity  $F_{\text{tot}}$  with the rate at which annihilations deposit energy  $F_{\text{ann}}$  within a given environment for each given anti-nugget. The total surface emissivity as well as the spectral density have been computed in [36]. It is mostly determined by photon emission from the electrosphere of the nugget, and it is given by

$$F_{\text{tot}} = \frac{dE}{dt dA} \simeq \frac{16}{3} \frac{T^4 \alpha^{5/2}}{\pi} \sqrt[4]{\frac{T}{m}}. \quad (3.4)$$

We should note that the spectrum of the emission is also known, and it is approximately flat in the extended region of frequencies with  $\omega \leq T$ . This should be contrasted with black body radiation, see [36] for the details.

In order to maintain the overall energy balance between the emission rate given by  $F_{\text{tot}}$  and annihilation rate given by  $F_{\text{ann}}$ , the nuggets must emit energy at the same rate that it is deposited through proton annihilation,  $F_{\text{tot}} \simeq F_{\text{ann}}$ .

Note that both the rate of emission and the rate of annihilation are expressed per unit surface area, so that the equilibrium condition is independent of the nuggets' size, and therefore of their average baryon number  $\langle B \rangle$ .

The rate of annihilation  $F_{\text{ann}}$  is

$$F_{\text{ann}} = 2 \text{ GeV} \cdot f(T, l) \cdot \eta(T, l) \cdot v(l) \cdot n_{\text{sun}}(l) \quad (3.5)$$

where  $2 \text{ GeV} \simeq 2 m_p$  is the energy liberated by proton annihilation,  $v(l)$  is the average speed of the nugget at the altitude  $l$  above the surface,  $n_{\text{sun}}(l)$  is the average nucleon density at the altitude  $l$ ,  $f(T) \leq 1$  is a suppression factor due to the possibility of reflection from the sharp quark-matter surface determined by the internal nugget's temperature  $T$ . Finally,  $\eta(T, l) \geq 1$  is an enhancement factor in the annihilation rate due to ionization of the surrounding plasma and very large charge of the anti-nugget  $Q$  which is build in during the motion of the anti-nuggets in the solar corona. We estimate the corresponding charge  $Q$  in Appendix A.

Now we want to present some simple numerical estimates for the altitude  $l \sim 3000$  km above the solar surface, where the density is sufficiently small and plasma effects cannot drastically change our estimate below. For order of magnitude estimates we take  $n_{\text{sun}}(l) \sim 10^{10} \text{ cm}^{-3}$ ,  $v \sim 10^{-3}c$ . Suppression factor  $f \simeq 0.1$  was estimated in [36] for low temperature and low density environment, while enhancement factor  $\eta(T)$  was not even considered previously in [36] as anti-nuggets were assumed to be neutral. It is very hard to estimate factor  $\eta(T)$  as it depends on many properties of the charged anti-nuggets and surrounding magnetized plasma. We presented few arguments in Appendix A that the corresponding enhancement factor  $\eta(T)$  due to the building of a large internal charge of the nugget could be very significant, especially in denser regions. For simplicity of this order of magnitude estimate we assume that these two factors approximately neutralize each other for the low density plasma for  $n_{\text{sun}}(l) \sim 10^{10} \text{ cm}^{-3}$ , i.e. we assume in eq. (3.6) that  $[f(T) \cdot \eta(T)] \simeq 1$ . Combining these numerical values, we obtain

$$F_{\text{ann}} \sim \frac{10^{17} \text{ GeV}}{\text{cm}^2 \cdot \text{s}} \cdot \left( \frac{f \cdot \eta}{1} \right) \cdot \left( \frac{v}{10^{-3}c} \right) \cdot \left( \frac{n_{\text{sun}}(l)}{10^{10}/\text{cm}^3} \right) \quad (3.6)$$

which must be compared with the total surface emissivity (3.4) which can be represented as follows

$$F_{\text{tot}} \sim 10^{17} \frac{\text{GeV}}{\text{cm}^2 \cdot \text{s}} \left( \frac{T}{10^6 \text{ K}} \right)^{4+1/4}, \quad T \sim 10^6 \text{ K}. \quad (3.7)$$

Taking the typical values for these parameters mentioned above and comparing (3.6) with (3.7) we arrive at an estimate of an intrinsic nugget temperature of  $T \simeq 10^6 \text{ K}$  for anti-nuggets travelling in the solar corona at an altitude of  $l \sim 3000 \text{ km}$ .

One should emphasize that the temperature  $T \simeq 10^6 \text{ K}$  which enters formulae (3.7) is the internal temperature of the anti-nuggets, and should not be confused with the surrounding plasma of the solar corona. The thermodynamical processes will eventually equilibrate the internal temperature (3.7) with the temperature in surrounding plasma. However, this is not

an instantaneous process, and there are many mechanisms in plasma which can transfer the energy (3.7) to the surrounding particles. We shall not discuss the corresponding equilibration mechanisms, as they are well beyond the scope of the present work. To simplify our analysis we just assume that the entire energy produced by the annihilating anti-nuggets will be eventually transferred to the surrounding plasma.

When the nuggets are slowly descending and the plasma density  $n_{\text{sun}}(l)$  is slowly increasing, the number of annihilation events (and corresponding energy deposit) is also increasing. It is expected that the rate of energy transfer from nuggets to the surrounding plasma will be also increasing<sup>5</sup> as time evolves. Precise estimations of all these effects which eventually should explain a complicated behaviour of the temperature  $T(l)$  as a function of altitude  $l$  are well beyond the scope of the present work and shall not be elaborated further.

The significance of this entire picture is that the anti-nuggets will be transferring their energy due to the annihilating processes to surrounding plasma with the spectrum and intensity which are consistent with the “mysterious puzzling features” listed in the Introduction. This is because the total intensity of the EUV emission is exclusively determined by the number of anti-nuggets captured by the Sun. It is estimated that the anti-nuggets will deposit their energy on the level of  $10^{-6}$  of the total solar luminosity according to (3.2) and (3.3), in agreement with the observations.

### 3.2 The annihilation pattern. The big picture.

The main assumption of the present work is that a finite portion of annihilation events have occurred before the anti-nuggets entered the dense regions of the Sun<sup>6</sup>. Just these annihilation events, according to our assumption, supply the energy source of the observed EUV radiation from the corona and the chromosphere.

The basic picture of the annihilation pattern can be viewed as follows. The capture parameter  $\gamma_{\odot}$  for the Sun is large. This unambiguously implies that a significant portion of the nuggets which are not on the head on collision trajectories with the Sun, nevertheless will be captured by the Sun according to (3.1). It also implies that a typical length of the nugget’s trajectory (where annihilation occurs) is quite long as it is of order of  $R_{\odot} \sim 10^6$  km as argued in Section 5, in huge contrast with collision of the AQN with Earth when  $\gamma_{\oplus} \ll 1$ . In the case with collision with the Earth a typical length of the AQN’s trajectory (where annihilation effectively occurs) would be of order of height of the Earth’s atmosphere  $\sim 10^2$  km.

As a result of this difference, the dominant portion of the energy due to the annihilation of the AQN in the Earth’s case will be deposited in the deep Earth’s underground regions while the main portion of the energy in the solar’s case will be mostly deposited in the corona/ chromosphere/ transition regions allowing the direct observations in form of the EUV and

---

<sup>5</sup>The energy transfer from nuggets to surrounding plasma in this case is not expressed by a simple expression (3.4) describing the photon emission by the nugget’s electrosphere at temperature  $T$ . The dominant mechanisms are expected to be much more complicated, and may include such processes as elastic and inelastic scatterings of the nugget’s degrees of freedom with protons and electrons from plasma, direct exchange processes, etc.

<sup>6</sup>We note that the complications related to a precise annihilation pattern (including the ionization of the nuggets and consequently, the complications related to the dynamics of the nuggets in the magnetic field) were absolutely irrelevant for analysis in refs.[39, 40] because the neutrinos will leave the system irrespectively of the precise altitude where annihilation event occurs. This is not the case with EUV radiation which can only leave the system if annihilation occurs above (or slightly below) the photosphere. This is because the EUV photons will be quickly thermalized if annihilation occurs in dense regions below the sun surface.

soft x-ray emissions from that regions. There are few additional arguments (such as high ionization of the solar corona) supporting this basic assumption. We elaborate on these issues in Section 5 where we argue that the Sun is an ideal place to study the AQN dark matter.

To recapitulate the main assumption of this work: we assume that the large portion of the AQN will loose their masses (their initial baryon charges) and their initial kinetic energies in Corona and Chromosphere before entering the dense photosphere region. At this point they finally get annihilated completely and cease to exist.

We estimate the corresponding time scale  $\tau$  where this most important portion of the annihilation occurs as follows.

$$\Delta B \sim n_{\text{sun}}(l) \cdot (\pi R_{\text{eff}}^2) \cdot v\tau \sim B, \quad (3.8)$$

where  $R_{\text{eff}}(l)$  is the effective size of an anti-nugget during the last moments of its existence. It does not coincide with the nugget's size  $R$  because the nuggets are electrically charged objects propagating in the ionized plasma, and the effective cross section for annihilation is much larger than  $R$ , see section A for the relevant estimates. Essentially this effective parameter accounts for complicated plasma effects (such as shock waves, bluster waves, etc) which could develop in unfriendly environment in vicinity of the moving nugget when a large number of particles from surrounding areas will be affected by the presence of the nugget, and will be involved in its dynamics. Eventually, these surrounding particles will have a chance for successful annihilation with anti-nugget, which is effectively described by a parameter  $R_{\text{eff}}(l)$  in eq. (3.8).

For very rough order of magnitude numerical estimates we assume  $n_{\text{sun}} \sim (10^{16} - 10^{18})\text{cm}^{-3}$  as a typical density of the region where anti-nuggets effectively complete their annihilation processes and cease to exist. For numerical estimates we assume  $R_{\text{eff}} \sim 0.1 \text{ cm}$  at this density as estimated in Appendix A. With these effective parameters in hands we arrive to the following numerical estimates for a typical time  $\tau$  during which the anti nugget will loose a large portion of its baryon charge before entering the deep interior regions of the Sun,

$$\frac{\Delta B}{B} \sim \left(\frac{10^{25}}{B}\right)^{\frac{1}{3}} \times \left(\frac{n_{\text{sun}}(l)}{10^{17}\text{cm}^{-3}}\right) \times \left(\frac{R_{\text{eff}}(l)}{10^{-1}\text{cm}}\right)^2 \times \left(\frac{v}{10^{-3}c}\right) \times \left(\frac{\tau}{10^2\text{s}}\right) \sim 1. \quad (3.9)$$

Numerical estimate (3.9) suggests that a typical time scale when a large portion of the annihilation occurs is of the order of  $10^2$  seconds. This estimate, of course, strongly depends on many numerical parameters used in (3.9) such as plasma density  $n_{\text{sun}}(l)$ , effective radius  $R_{\text{eff}}(l)$ , and the initial baryon charge  $B$  of an anti-nugget.

It is quite possible that the unusual features of the the transition region (such as very fast rise of the temperature within 10–100 km) are intimately related to these annihilation events. It is also possible that at the altitude of  $l \sim 2000 \text{ km}$  the nuggets are losing their kinetic energy, their baryonic charge, their mass very efficiently when they approach the photosphere from the higher elevations. It is also very likely that the anti-nuggets may loose their entire baryon charge  $B$  before entering the dense regions of the photosphere, which is precisely our main assumption formulated above and qualitatively supported by the estimate (3.9).

It is not our goal to speculate on these and other related questions, which are obviously beyond the scope of the present work. The only comment we would like to make here is that the estimate (3.9) on the annihilation pattern is quite sensitive to a specific size of the nugget, in contrast with our previous estimates (3.2), (3.3) and (3.7) which are very generic features

of the framework rather than specific properties of a model. In fact, we present the model-dependent estimate (3.9) in this subsection exclusively with a purpose to identify the large events of annihilation in the corona/chromosphere (when  $B$  could be as large as  $B \gtrsim 3 \cdot 10^{26}$ ) with the observed and previously analyzed nanoflares as advocated in section 4.

## 4 Observation of nanoflares as evidence for anti-nuggets in Corona

The main claim of this work is that the corona and the chromosphere might be powered by the annihilation of the dark matter anti-nuggets. All our arguments supporting this claim, up to this section, were based on the consideration of the total energy budget estimates (3.2) and the typical spectral properties (3.7). Both these observables are not sensitive to a specific size distribution of the nuggets, as it has been already mentioned previously.

In this section we want to make one step further and identify the annihilation events of the anti-nuggets with the previously studied “nanoflares”, which belong to the burst-like solar activity. Therefore, this section is much more speculative, in comparison with previous discussions of section 3, as it includes an additional assumption in form of identification of the AQN annihilation events with observed “nanoflares”.

However, before we elaborate on this possible connection between the AQN annihilation events and nanoflares we want to make a short historical detour in section 4.1 on the nanoflares and their role in physics of corona as studied in previous works. In section 4.2 we present few arguments (based on various observations) supporting our interpretation that sufficiently energetic annihilation events of the anti-nuggets with  $B \gtrsim 3 \cdot 10^{26}$  are behind the observed nanoflares. Smaller nanoflares are not directly observed due to the instrumental threshold. In section 4.3 we make few comments on possible future development. We also overview in section 4.3 some recent results related to the modelling of the plasma heating in corona when the nanoflares play the key role in analysis.

### 4.1 Few historical remarks on nanoflares

The term “nanoflare” has been introduced by Parker in 1983 [7]. Later on this term has been used in series of papers by Benz and coauthors [41–45] to advocate the idea that precisely these small “micro-events” might be responsible for the heating of the quiet solar corona. We want to list below few important features which have been discussed in previous works [41–45] before we present our original arguments suggesting that these nanoflares have the same features as annihilation events of anti nuggets in the corona.

We follow the definition suggested in [45] and refer to nanoflares as the “micro-events” in quiet regions of the corona, to be contrasted with “micro flares” which are significantly larger in scale and observed in active regions. The term “micro-events” refers to a short enhancement of coronal emission in the energy range of about  $(10^{24} - 10^{28})$ erg. One should emphasize that the lower limit gives the instrumental threshold observing quiet regions, while the upper limit refers to the smallest events observable in active regions. Below we list most important features of nanoflares which became possible by observing EUV iron lines with SoHO/EIT. The main features are:

- 1 The coronal emission measure observed in EUV iron lines fluctuates locally at time scales of few minutes in a majority of pixels including even the intracell regions of the quiet corona;
- 2 It was reported  $1.1 \times 10^6$  events per hour over the whole Sun for SoHO/EIT observations [42, 44];
- 3 The energy output observed by EIT on the SoHO satellite is of order of 10% of the total

radiative output in the same region [44];

**4** To reproduce the measured radiation loss, the observed range of nano flares (having a lower limit at about  $3 \cdot 10^{24}$ erg is due to the instrumental threshold) needs to be extrapolated to energies as low as  $10^{22}$ erg and in some models even to  $10^{20}$ erg, see table 1 in ref.[43];

**5** nanoflares and micro-flares appear in different ranges of temperature and emission measure, see Fig.3 in ref. [45]. While the instrumental limits prohibit observations at intermediate temperatures, nevertheless the authors of ref. [45] argue that “the occurrence rates of nanoflares and micro-flares are so different that they cannot originate from the same population”;

**6** Time measurements of many nanoflares demonstrate the Doppler shift with a typical velocities (250-310) km/s, see Fig.5 in ref. [41]. The observed line width in OV of  $\pm 140$  km/s far exceeds the thermal ion velocity which is around 11 km/s [41].

## 4.2 Nanoflares as the annihilation events of the anti-nuggets

It is very tempting to identify the nanoflares reviewed in previous subsection 4.1 with the events of annihilation of the anti-nuggets inside the solar corona. Before we present our arguments supporting this identification we would like to make the following few generic comments.

We describe the nuggets in terms of the baryon charge  $B$ . Annihilation of a single baryon charge produces the energy about 2 GeV which is convenient to express in terms of the conventional units as follows,

$$1 \text{ GeV} = 1.6 \cdot 10^{-10} \text{ J} = 1.6 \cdot 10^{-3} \text{ erg.} \quad (4.1)$$

This relation suggests that the current instrumental threshold of a nanoflare characterized by the energy  $\sim 10^{24}$  erg corresponds to the (anti) baryon charge of the nugget  $B \approx 3 \cdot 10^{26}$ . Anti-nuggets with smaller  $B$  are present in the corona but are considered as the sub-resolution events. This claim follows from item 4 above which suggests that nanoflares with sub-resolution energies must be present in the system to reproduce the measured radiation loss.

Indeed, according to item 4 from previous subsection 4.1, in order to reproduce the observed radiation loss the energy of nanoflares must be extrapolated from sub-resolution events with energy  $3.7 \cdot 10^{20}$  erg to the observed events interpolating between  $(3.1 \cdot 10^{24} - 1.3 \cdot 10^{26})$  erg. For a different extrapolation model used in [43] the energy varies from  $(9.8 \cdot 10^{21} - 6.3 \cdot 10^{25})$  erg. This energy window corresponds to the (anti) baryon charge of the nugget  $10^{23} \leq |B| \leq 4 \cdot 10^{28}$  (or  $3 \cdot 10^{24} \leq |B| \leq 2 \cdot 10^{28}$  for a different extrapolation model used in [43]).

We want to emphasize that this window of acceptable extrapolations is largely overlapped with all presently available and independent constraints on such kind of dark matter masses and baryon charges  $B$ , see e.g. [18, 46] for review<sup>7</sup>. To reiterate the same claim: the allowed window for the baryon charge  $B$  (and corresponding radiation energy due to annihilation of the anti-nuggets) is perfectly consistent with all presently available constraints.

---

<sup>7</sup>The smallest nuggets with  $B \sim (10^{23} - 10^{24})$  naively contradict to the constraints cited in [46]. However, the corresponding constraints are actually derived with the assumption that nuggets with a definite mass (smaller than 55g) saturate the dark matter density. In contrast, we assume that the peak of the nugget’s distribution corresponds to a larger value of mass, while the small nuggets represent a tiny portion of the total dark matter density. The same comment also applies to the larger masses excluded by Apollo data as reviewed in [18]. Large nuggets with  $B \sim 10^{28}$  do exist, but represent a small portion of the total dark matter density.



According to item **5** above the nanoflares are distributed very uniformly in quiet regions, in contrast with micro-flares which are much more energetic and occur exclusively in active areas. It is consistent with the dark matter interpretation as the anti-nuggets annihilation events (identified with nanoflares) should be present in all areas irrespectively to the activity of the Sun. At the same time the micro-flares are originated in the active zones, and therefore cannot be uniformly distributed.

The presence of the large Doppler shift with a typical velocities (250-310) km/s as mention in item **6** above can be understood within the dark matter interpretation of the nanoflares. Indeed, the typical velocities of the nuggets entering the solar corona is about  $\sim 300$  km/s, which is very close to the measured Doppler shift.

The observed iron lines as mentioned in item **1** is also easy to interpret within our identification of the nano flares with the annihilating anti-nuggets. Indeed, according to the estimate (3.9) the typical event with  $B \sim (10^{27} - 10^{28})$  corresponding to the observed nanoflares may last few minutes. This is the time scale needed for anti-nuggets to completely annihilate their baryon charge. This time-scale is obviously highly sensitive to the altitude  $l$  where annihilation happens and to the initial baryon charge  $B$  of the anti-nuggets. However, a very reasonable order of magnitude estimate (3.9) once again supports our reasoning that the nanoflares can be identified with the annihilation events of dark matter anti-nuggets.

The measured energy and number of recorded events according to items **2** and **3** above represent only small factor of the total radiation energy in the same solar region. The interpretation of this "apparent deficiency" is also very straightforward within our framework. Indeed, only a small portion of the nuggets are sufficiently large to produce the events with the energies above the instrumental threshold which can be recorded. Smaller events are likely to occur in the corona as discussed above (see the paragraph after eq. (4.1) with estimates on the window for  $B$ ), and likely to contribute to the total solar radiative output in this energy range, but they are not recorded due to insufficient resolution of the current instruments.

### 4.3 Recent advances and Future development

In this subsection we make few comments on recent results on nanoflares and their role in the heating mechanisms of corona. We also comment on possible future development which may support our interpretation of the nanoflares as the AQN annihilation events.

It would be highly desirable to estimate the baryon charge distribution of the AQNs from the theoretical side, irrespectively to the solar physics. In this case one could estimate the corresponding energy distribution of the nanoflare events in the solar corona as the baryon charge of the AQN is unambiguously translated into the energy of the nanoflares. This statement can be formally expressed as follows

$$dN \sim B^{-\alpha} dB \sim W^{-\alpha} dW, \quad (4.2)$$

where  $dN$  is the number of the nanoflare events per unit time with energy between  $W$  and  $W + dW$  which occur as a result of complete annihilation of the anti-nuggets carrying the baryon charges between  $B$  and  $B + dB$ . These two distributions are tightly linked as these two entities are related to the same AQN objects when the unit baryon charge generates annihilation energy (4.1) according to our interpretation of the observed nanoflare events. Unfortunately, the corresponding theoretical estimates of the distribution  $dN/dB$  are very hard to carry out in spite of the fact that we are dealing with the standard model (SM) physics with no new fundamental parameters outside the SM physics.



Indeed, one encounters two major difficulties in the path to produce such a theoretical estimate. First of all, the initial axion domain wall size distribution of the closed bubbles (which eventually form the nuggets) is unknown as discussed in the original paper [19] devoted to the formation mechanism of the AQNs. Only the total baryon charge hidden in all nuggets and anti-nuggets is known as it is expressed in terms of the dark matter density. In practice the problem becomes even more complicated because the axion domain wall bubble evolution is accompanied by the process of accumulation of the baryon charge in its bulk as discussed in [19]. It is very hard to predict the outcome of these complicated processes depending on the size distribution. Needless to say that even the phase diagram at  $\theta \neq 0$  when the formation of the AQN occurs is still unknown, and the QCD lattice numerical simulations run into the fundamental obstacle as a result of the so-called sign problem when  $\theta$  parameter and chemical potential  $\mu$  assume some non-zero values.

The second major barrier to produce a theoretical estimate (4.2) irrespectively to the solar physics is a lack of understanding of the evolution of the AQN from the moment of formation at  $T \sim 1$  GeV to the present cold Universe. The problem here is that the nuggets evolve in very unfriendly environment in plasma when all relevant parameters  $T, \mu, \theta$  were nonzero and some (smaller) nuggets may not survive the evolution, while other (larger) nuggets may drastically change their initial baryon charge as a result of annihilation and accretion processes. All these effects, are obviously order of one effects (as everything else in nuclear physics), and drastically influence the size distribution (4.2). This is precisely the reason why any quantitative estimates of the size distribution are very hard to carry out. It should be contrasted with our total energy budget estimates (3.2) and the typical spectral properties (3.7) which are expressed in terms of the observable parameters (such as dark matter density) and represent very solid predictions of this framework as they are not sensitive to the size distribution.

To reiterate: it is not feasible at present time to make any considerable progress in theoretical estimates of the baryon charge distribution  $dN/dB$  due to the two major problems outlined above.

Fortunately, on the observational (data analysis) side with the estimates  $dN/dW$  some progress can be made. In fact, we want to make few comments on the recent papers [47–52] related to the nanoflares and corresponding statistical analysis of the observations in the corona<sup>8</sup>. In most studies the term “nanoflare” describes a generic event for any impulsive energy release on a small scale, without specifying its cause, see review paper [47] and preprint [48] with references on recent activities in the field. In other words, in most studies the hydrodynamic consequences of impulsive heating (due to the nanoflares) have been used without discussing their nature. In contrast, in our work we do not discuss the hydrodynamics, but rather we address precisely the question on the origin of the energy responsible for coronal heating problem. Our total energy budget estimate (3.2) in the AQN model suggests that the nuggets might be responsible for coronal heating as the corresponding estimate is consistent with the observed luminosity (1.1).

With these preliminary remarks it is fair to say that there is some agreement between different groups [47–52] that nanoflares may play a dominate role in heating of solar corona. For example, for the typical parameters assumed in [49] the authors conclude that in order to reproduce the observations the nanoflares must have typical energies  $\langle W \rangle$  and the frequencies

---

<sup>8</sup>I thank anonymous referee for the relevant comments and pointing out to some important references related to the recent nanoflare observations.

of appearance  $dN/dt$  as follows [49]:

$$\langle W \rangle \simeq 10^{23} \text{ erg}, \quad \left\langle \frac{dN}{dt} \right\rangle \simeq (10^3 - 10^4) \text{ s}^{-1}. \quad (4.3)$$

The product  $\langle W \rangle \cdot \langle \frac{dN}{dt} \rangle$  obviously shows that (4.3) is perfectly consistent with previous analysis [41–45] overviewed in subsection 4.1 and with our estimate (3.2) based on the AQN dark matter model. At the same time, there are some disagreements between different groups on spectral properties  $dN/dW$  of the flares expressed in terms of power-law index  $\alpha$  as defined in (4.2).

In particular, the authors of ref. [49] claim that the best fit to the data is achieved with  $\alpha \simeq 2.5$  with typical energies (4.3), while numerous attempts to reproduce the data with  $\alpha < 2$  were unsuccessful. It should be contrasted with another analysis [51] which suggests that  $\alpha \simeq 1.2$  for events below  $W \leq 10^{24}$  erg, and  $\alpha \simeq 2.5$  for events above  $W \geq 10^{24}$  erg. Analysis [51] also suggests that the change of the scaling (the position of the knee) occurs at energies close to  $\langle W \rangle \simeq 10^{24}$  erg, which roughly coincides with the maximum of the energy distribution, see Fig.7 in [51].

One should also remark on a different analysis [50] which includes RHESSI data with the energies range from  $10^{26}$  erg to  $10^{30}$  erg with the median being about  $\langle W \rangle \simeq 10^{28}$  erg. It has been noted in [50] that it is conceivable that the distribution of all flares follows a single power-law with  $\alpha \simeq 2$ , which might suggest a common origin for all flares, see Fig. 18 in [50]. Of course, the comparison between different components of the energy distribution is a highly nontrivial procedure as it includes comparison of the data produced by the different instruments with specific instrumental effects. Furthermore, different components of the energy distribution covers different phases of the solar cycle.

Our comment on the proposal of ref. [50] (that all flares follow a single power-law with  $\alpha \simeq 2$ ) can be formulated as follows. It still requires some additional arguments and analysis to see that the gaps between different energy components presented on Fig. 18 in [50] are indeed the instrumental, and not the physical effects. Furthermore, the proposal of ref. [50] is not easy to reconcile with the comment made in [45] that “the occurrence rates of nano flares and micro flares are so different that they cannot originate from the same population”. This proposal is also difficult to reconcile with results of ref.[51] where the “knee” in the spectrum is observed when the power law changes from  $\alpha \simeq 2.5$  for high energies to  $\alpha \simeq 1.2$  for low energies. From the AQN dark matter perspectives the nanoflares and microflares are considered to be very different types of events, with the only possible connection between them is that the anti-nuggets could play the role of the *triggers* activating the magnetic reconnection of *preexisted* magnetic fluxes in active regions (which may generate the larger flares), as remarked in item 3 in Section 6.

We conclude this section with the following remarks. Our proposal (that the observed nanoflares can be interpreted as the annihilation events of the anti-nuggets) is consistent with available observations and data analysis, including the independent constraints on the axion mass  $m_a$  and the baryon charge  $B$  as mentioned in Section 4.2. While a theoretical estimate for the baryon charge distribution  $dN/dB$  defined by (4.2) is not feasible at the present time, some further progress in modelling of the  $dN/dW$  distribution (which is proportional to  $dN/dB$  within the AQN model) is a achievable, in principle, as it is based on conventional technical tools such as magnetohydrodynamical simulations and data analysis, as discussed in Section 4.3. Furthermore, the future advances in the axion search experiments, see recent reviews [24–31], will further constraint the axion mass  $m_a$ . These constraints may narrow

the window for the baryon charges  $B$  of the nuggets within the framework of the AQN dark matter model. Consequently, the narrowing window for allowed  $B$  can be translated into the constraints on the possible energy window for the nanoflare events as discussed in Section 4.2.

## 5 Sun as an ideal place to study AQN dark matter model

In this section we want to argue that the solar environment has a number of special features which make the Sun to be a perfect place to study the AQN dark matter model overviewed in Section 2.

In the previous studies [32–38] it has been argued that the AQN dark matter model is consistent with all presently available observations of the galactic radiation. Furthermore, there is a number of frequency bands where some excess of emission was observed, and this model may explain some portion, or even entire excess of the observed radiation in these frequency bands. At the same time, nearby galaxies are essentially not sensitive to this type of dark matter as argued in [53, 54]. It has been also previously argued [55, 56] that the large scale cosmic ray detectors are capable of observing quark nuggets passing through the earth’s atmosphere, see also short review paper [18].

In contrast with those previous studies of the nuggets passing through the earth’s atmosphere, our present proposal is to use the solar corona background in order to investigate the AQN dark matter model. This proposal has many advantages in comparison with the ground based searches on Earth due to the following main reasons. The earth’s atmosphere is much smaller in height than the solar atmosphere. Furthermore, the solar parameter  $\gamma_{\odot}$  as defined by eq. (3.1) is numerically large. This implies that a large portion of the nuggets which are not on head on collision trajectories nevertheless will be captured by the sun. It also implies that a typical length of the nugget’s trajectory is of order of  $R_{\odot}$ , i.e.  $\sim 10^6$  km.

It should be contrasted with collision with the Earth when  $\gamma_{\oplus} \ll 1$ , and therefore only the nuggets with head on trajectories will be captured by the Earth. A typical length of the nugget’s trajectory in this case of head on collisions is of order of height of the earth’s atmosphere  $\sim 10^2$  km, rather than  $R_{\oplus}$ .

Another important distinct feature is that the solar atmosphere is the mixture of the light elements such as hydrogen and helium which can be easily annihilated by the anti-nuggets. It should be contrasted with earth’s atmosphere which is a mixture of relatively heavy elements such as nitrogen and oxygen which are most likely to be reflected by the anti-nuggets rather than annihilated by them. Therefore, in spite of the fact that the column density of the earth’s atmosphere is much higher than the column density of the solar atmosphere, the number of the annihilation events is expected to be much higher for the Sun in comparison with the Earth as a result of these two distinct features.

Furthermore, the solar atmosphere is highly ionized system, in contrast with the earth’s atmosphere, and therefore, the annihilation processes are much more efficient in the solar environment in comparison with the Earth environment due to large number of protons from plasma accompanying the anti-nuggets as a result of the Debye screening. This effect drastically increases the effective radius  $R_{\text{eff}}$  of the interaction of the anti-nuggets as described in Section 3.

These few distinct features lead to the profound observational consequences: an anti-nugget entering the earth’s atmosphere will be losing only a tiny portion of its baryon charge before hitting the ground and entering the earth’s dense underground regions, after which the direct observable consequences are very hard to recover.

It should be contrasted with an anti-nugget entering the solar corona in which case the anti-nugget may completely lose its baryon charge even before entering the dense regions of the photosphere as argued in section 3. As a result of these differences, most of the energy in the Earth's case will be deposited in the deep earth's underground regions while the major portion of the energy in the solar's case will be mostly deposited in the corona/ chromosphere/ transition regions allowing the direct observations in form of the EUV and soft x-ray emissions by EIT and similar instruments. This makes the solar atmosphere to become an ideal environment to study the AQN dark matter model.

## 6 Concluding remarks and Wild speculations.

The main claim of the present work is that the observed EUV and soft x-rays in the Corona might be originated from the AQNs proposed in [9] for completely different purposes. The total solar intensity (3.2), the spectrum and estimated temperature (3.7) are fully consistent with this proposal<sup>9</sup>.

We also conjectured in section 4 that the events of annihilations of the AQNs can be interpreted as the previously studied nanoflare events. This conjecture on identification of these two (naively different) entities is supported by a number of observations listed in section 4.1 as interpreted in section 4.2 in terms of the annihilation events of the anti-nuggets in the corona /TR/ chromosphere.

We list below a number of observed (but not understood) phenomena in many systems, which could be related to the dark matter AQNs studied in the present work. The corresponding list, which is obviously far from complete, in particular, includes:

1. There are some unexplained events, such as the Tunguska-like events when no fragments or chemical traces have ever been recovered. We speculate that such unusual events might be the result of the collision of the anti-nugget with Earth, as it was previously mentioned in the original paper [9].

2. There are some unexplained seismic-like events, similar to the one discussed in [57]. Such events could also be related to the dark matter nuggets advocated in this work.

3. The conventional viewpoint is that the solar flares occur as a result of the magnetic reconnections. There are many known controversial elements in implementation of this idea which shall not be discussed here. The only original comment we would like to make here is that the quark anti-nuggets could play the role of the *triggers* activating the magnetic reconnection of preexisted fluxes. This is because the nuggets locally deposit the energy which may produce a sufficiently strong local disturbance initiating the flares. It may also speed up the magnetic reconnection which is known to be a crucial controversial element in corresponding computations, see textbook [58] for review.

4. There is a number of studies on the galactic scales suggesting that the DM, in fact, couples to the luminous matter. In particular, in ref. [59] it has been argued that the observed correlations between the dark and luminous components is very hard to explain in a conventional dark matter scenario. Our original comment here is that the AQN dark matter model is a natural candidate which is, in principle, capable to resolve these puzzles as the nuggets are actually made of strongly interacting quarks and gluons. Furthermore, both components of matter (visible and dark) have the same origin, have been formed at the

---

<sup>9</sup>The corresponding estimates were based on the assumption explicitly formulated in the first paragraph in section 3.2.

same QCD transition, and both proportional to the same fundamental dimensional parameter  $\Lambda_{\text{QCD}}$  as reviewed in Section 2.

5. A very different study of a number of correlations in the Sun and its planets strongly suggest a presence of “invisible matter” [60]. It would be very interesting to see if the AQNs are capable to play the role of the “invisible matter” postulated in [60].

We conclude this work with following proposals for the futures studies which may further support (or rule out) this mechanism when the energy supply to the Corona is provided by the AQNs as determined by the dark matter density  $\rho_{\text{DM}} \sim 0.3 \text{ GeVcm}^{-3}$  according to estimate (3.2). This mechanism automatically, without adjusting of any parameters, generates the observed fraction  $\sim 10^{-6}$  of the total solar luminosity emitted in the form of the EUV and soft x-rays.

- First of all, a similar EUV and soft x-ray radiation discussed in the present work observed in the Sun must be present in many similar stars, though the intensity and the spectral properties are highly sensitive to the specific features of stars and their positions in the galaxy. Such a radiation indeed has been observed in many systems, see [1] for review. A detail studies of the EUV and x-ray radiation (especially in quiet stellar’s regions) in different types of stars is highly desirable as it may shed some light on understanding of different types of energy sources responsible for the corona heating for variety of stars. The intensity and spectral properties of the radiation must obviously depend on internal structure of a star under study, as well as the outer dark matter density  $\rho_{\text{DM}}(r)$  which itself strongly depends on position of the star with respect to the galactic center.

In particular, if the future observations suggest that the EUV and x-ray radiation from stars is not sensitive to surrounding dark matter density  $\rho_{\text{DM}}(r)$  it would unambiguously rule out our proposal as the number of annihilation events (and therefore the intensity of the EUV radiation) is directly proportional to the dark matter density in vicinity of a specific star according to the basic formula (3.2).

- Secondly, the observation of the nanoflares with SoHO/EIT has a specific instrumental threshold  $\sim 3 \cdot 10^{24}$  erg. A very modest improvements in resolution (on the level of factor 3 or so) should result in corresponding increase of the rate of the observed nanoflares, which we identify with annihilation events of anti-nuggets with solar material as described in section 4. The corresponding measurements would provide the information about the nugget’s size distribution (4.2), and may resolve some discrepancies between different group modelling and analyzing the data as mentioned in section 4.3. It is very important to perform the corresponding analysis by separating the nanoflares in quiet regions from active regions to avoid any mis-identification of the nanoflares with unrelated micro-events which receive their energy as a result of the alternative sources such as the magnetic reconnections in active regions.

In particular, if the future observations show that there is a sharp cutoff (or other drastic changes) in the nanoflare distribution somewhere in the range  $(10^{22} - 10^{24})$  erg it would unambiguously rule out the proposal because the nugget’s baryon charge  $B$  must be continuously extended to sufficiently low  $B \sim 10^{24}$  as the average baryon charge of the the AQNs is estimated to be in the range  $\langle B \rangle \sim 10^{25}$  as mentioned at the end of section 2.

## Acknowledgements

I am thankful to Konstantin Zioutas for inviting me to the Patras workshop 2017 (Thessaloniki, May 2017) where this project was started. I am also grateful to him for our collabo-

ration during the initial stage of this project. I am also indebted to Konstantin for teaching me about the solar system and its mysterious behaviour. I am also thankful to Kyle Lawson for useful comments. This research was supported in part by the Natural Sciences and Engineering Research Council of Canada.

## A Few technical characteristics of the anti-nuggets at $T \neq 0$

The main goal of this Appendix is to provide few simple qualitative estimates which have been used in the main text.

First, we estimate the electrical charge of the anti nuggets when they enter the solar corona. The basic idea of the estimate is as follows. The total neutrality of the nuggets in the model is supported by electrosphere made of leptons (positrons for the anti-nuggets). For non-zero intrinsic nugget's temperature  $T \neq 0$  a small portion of the loose positrons will be stripped off from the anti-nuggets. As a result the anti-nuggets will esquire a non vanishing negative electric charge  $Q$ . To estimate this charge  $Q$  one can use the electro-sphere density profile function  $n(r)$  by removing the contribution of the region of loosely bounded positrons with low momentum  $p^2 \leq 2m_e T$ .

The corresponding computations can be carried out using the electro-sphere density profile function computed in [35] within the Thomas-Fermi approximation<sup>10</sup>. For the present work it is sufficient to use the non-relativistic approximate expression for the profile function  $n(r)$  given in [36]. The corresponding computation leads to the following estimate for  $Q$ :

$$Q \simeq 4\pi R^2 \int_{\frac{1}{\sqrt{2m_e T}}}^{\infty} n(z) dz \sim \frac{4\pi R^2}{2\pi\alpha} \cdot \left(T\sqrt{2m_e T}\right). \quad (\text{A.1})$$

For the numerical estimate we assume  $R \sim 10^{-5}$  cm and  $T \simeq 100$  eV according to eq. (3.7). In this case  $Q \sim 10^8$  which represents very tiny portion in comparison with the baryon charge  $B \sim 10^{25}$  hidden in the anti-nugget, i.e.  $(Q/B) \ll 1$ . Nevertheless, the charge  $Q$  plays an important role in the dynamics of the anti-nuggets as they become subject to the strong electric and magnetic forces, which are ubiquitous in the Sun atmosphere.

The second parameter which was used in our estimates (3.8), (3.9) in the main text is the effective size  $R_{\text{eff}}(l)$  of a nugget when it moves in the hot ionized plasma. As explained in the main text this environment may drastically affect the annihilation rate due to a number of many body plasma phenomena mentioned after eq. (3.8). The same scale  $R_{\text{eff}}(l)$  essentially determines how the generated energy (due to the annihilation processes) is transferred to the surrounding plasma. One can treat the parameter  $R_{\text{eff}}(l)$  as a typical scale which counts the number of particles from plasma  $\sim n_{\text{sun}}(l)R_{\text{eff}}^3(l)$  which effectively participate in the processes of annihilation and energy transfer from the nugget to surrounding plasma.

The simplest and very rough way to estimate the corresponding effective size  $R_{\text{eff}}$  is to approximate an effective Coulomb cross section by assuming that a typical momentum transfer is order of the temperature of the surrounding plasma,  $|q| \sim T$ , i.e.

$$\pi R_{\text{eff}}^2 \sim \frac{Q^2 \alpha^2}{q^2} \sim \frac{Q^2 \alpha^2}{T^2}. \quad (\text{A.2})$$

<sup>10</sup>The profile function computed in [35] describes well the interpolation between the non-relativistic and relativistic regimes. It was important for relating the intensities of the galactic of 511 keV line with (1 – 20) MeV diffuse photons which resulted from annihilation of visible electrons with non-relativistic positrons (511 keV line) and relativistic positrons (in (1 – 20) MeV range) from the electro-sphere.



Using numerical estimates for  $Q$  from (A.1) and for temperature  $T \simeq 10^6\text{K}$  we arrive to the following estimate for  $R_{\text{eff}}$  which effectively determines the size of the system

$$R_{\text{eff}} \sim 0.1 \text{ cm} \quad \text{for } Q \sim 10^8 \quad \text{and } T \simeq 10^6\text{K}. \quad (\text{A.3})$$

Precisely this estimate has been used in formula (3.9) in the main text.

One should emphasize that  $R_{\text{eff}}$  estimated above is drastically different from our previous studies (when the relevant size coincides with the radius of the nugget  $R$ ) reviewed in section 2 due to two reasons. First, the anti-nuggets are the charged objects according to (A.1). Secondly, the charged anti-nuggets are propagating in ionized plasma which strongly affects the annihilation rate as well as the energy transfer rate, as mentioned above. These features make the solar atmosphere to become an unique place to study this type of dark matter, as discussed in section 5.

## References

- [1] P. Testa, S.H. Saar, J.J. Drake, Phil. Trans. R. Soc. **A373**, 20140259 (2015) (arXiv:1502.07401v1).
- [2] R.G. Fowler, J. Hashemi, Nature **230**, 518 (1970).
- [3] N. D’Angelo, Solar Phys. **7**, 321 (1969).
- [4] W.A. Whitaker, ApJ. **137**, 914 (1963).
- [5] L. DiLella, K. Zioutas, Astroparticle Physics, **19**, 145 (2003). [arXiv:astro-ph/0207073v1].
- [6] K. Zioutas, CERN Courier, May 2008 (<http://cerncourier.com/cws/article/cern/34259>).
- [7] E.N. Parker, ApJ, **264**, 642 (1983); *ibid.* **330**, 474 (1988).
- [8] H.P. Warren, I. Ugarte-Urra, D.H. Brooks, J.W. Cirtain, D.R. Williams, H. Hara, PASJ. **59**, S675 (2007).
- [9] A. R. Zhitnitsky, JCAP **0310**, 010 (2003) [hep-ph/0202161].
- [10] E. Witten, Phys. Rev. D **30**, 272 (1984).
- [11] E. Farhi and R. L. Jaffe, Phys. Rev. D **30**, 2379 (1984). doi:10.1103/PhysRevD.30.2379
- [12] A. De Rujula and S. L. Glashow, Nature **312**, 734 (1984). doi:10.1038/312734a0
- [13] J. Madsen, Lect. Notes Phys. **516**, 162 (1999) [astro-ph/9809032].
- [14] Y. Aoki, G. Endrodi, Z. Fodor, S. D. Katz and K. K. Szabo, Nature **443**, 675 (2006) [hep-lat/0611014].
- [15] C. Alcock and E. Farhi, Phys. Rev. D **32**, 1273 (1985).
- [16] D. H. Oaknin and A. Zhitnitsky, Phys. Rev. D **71**, 023519 (2005) [hep-ph/0309086].
- [17] A. Zhitnitsky, Phys. Rev. D **74**, 043515 (2006) [astro-ph/0603064].
- [18] K. Lawson and A. R. Zhitnitsky, Snowmass 2013 e-Proceedings, arXiv:1305.6318 [astro-ph.CO].
- [19] X. Liang and A. Zhitnitsky, Phys. Rev. D **94**, 083502 (2016) [arXiv:1606.00435 [hep-ph]].
- [20] S. Ge, X. Liang and A. Zhitnitsky, Phys. Rev. D **96**, no. 6, 063514 (2017) [arXiv:1702.04354 [hep-ph]].
- [21] R. D. Peccei and H. R. Quinn, Phys. Rev. D **16**, 1791 (1977);  
S. Weinberg, Phys. Rev. Lett. **40**, 223 (1978);  
F. Wilczek, Phys. Rev. Lett. **40**, 279 (1978).



- [22] J.E. Kim, Phys. Rev. Lett. **43** (1979) 103;  
M.A. Shifman, A.I. Vainshtein, and V.I. Zakharov, Nucl. Phys. **B166** (1980) 493(KSVZ-axion).
- [23] M. Dine, W. Fischler, and M. Srednicki, Phys. Lett. **B104** (1981) 199;  
A.R. Zhitnitsky, Yad.Fiz. **31** (1980) 497; Sov. J. Nucl. Phys. **31** (1980) 260 (DFSZ-axion).
- [24] K. van Bibber and L. J. Rosenberg, Phys. Today **59N8**, 30 (2006);
- [25] S. J. Asztalos, L. J. Rosenberg, K. van Bibber, P. Sikivie, K. Zioutas, Ann. Rev. Nucl. Part. Sci. **56**, 293-326 (2006).
- [26] Pierre Sikivie, Lect. Notes Phys. **741**, 19 (2008) arXiv:0610440v2 [astro-ph].
- [27] G. G. Raffelt, Lect. Notes Phys. **741**, 51 (2008) [hep-ph/0611350].
- [28] P. Sikivie, Int. J. Mod. Phys. A **25**, 554 (2010) [arXiv:0909.0949 [hep-ph]].
- [29] L. J. Rosenberg, Proc. Nat. Acad. Sci. (2015),
- [30] P. W. Graham, I. G. Irastorza, S. K. Lamoreaux, A. Lindner and K. A. van Bibber, Ann. Rev. Nucl. Part. Sci. **65**, 485 (2015) [arXiv:1602.00039 [hep-ex]].
- [31] A. Ringwald, arXiv preprint (2016) [arXiv:1612.08933 [hep-ph]]
- [32] D. H. Oaknin and A. R. Zhitnitsky, Phys. Rev. Lett. **94**, 101301 (2005),  
[arXiv:hep-ph/0406146].
- [33] A. Zhitnitsky, Phys. Rev. D **76**, 103518 (2007) [astro-ph/0607361].
- [34] K. Lawson and A. R. Zhitnitsky, JCAP **0801**, 022 (2008), [arXiv:0704.3064 [astro-ph]].
- [35] M. M. Forbes, K. Lawson and A. R. Zhitnitsky, Phys. Rev. D **82**, 083510 (2010).  
[arXiv:0910.4541 [astro-ph.GA]].
- [36] M. M. Forbes and A. R. Zhitnitsky, Phys. Rev. D **78**, 083505 (2008) [arXiv:0802.3830  
[astro-ph]].
- [37] M. M. Forbes and A. R. Zhitnitsky, JCAP **0801**, 023 (2008) [astro-ph/0611506].
- [38] K. Lawson and A. R. Zhitnitsky, Phys. Lett. B **724**, 17 (2013) [arXiv:1210.2400 [astro-ph.CO]].
- [39] P. W. Gorham and B. J. Rotter, Phys. Rev. D **95**, no. 10, 103002 (2017) [arXiv:1507.03545  
[astro-ph.CO]].
- [40] K. Lawson and A. R. Zhitnitsky, Phys. Rev. D **95**, no. 6, 063521 (2017) [arXiv:1510.07646  
[astro-ph.HE]].
- [41] S. Krucker, A. O. Benz, Solar Phys. **191**, 341, (2000).
- [42] S. Krucker, A. O. Benz, ASP Conference Series, Vol. **200**, (2001) P. Brekke, B. Fleck, and J. B. Gurman eds, [arXiv:astro-ph/0012106].
- [43] U. Mitra Kraev, A. O. Benz, A&A, **373**, 318, (2001).
- [44] A. O. Benz, S. Krucker, Astrophys. J., **568**, 413, (2002).
- [45] A. O. Benz, P. Grigis, Advances in Space research, **32**, 1035 (2003) [arXiv:astro-ph/0308323].
- [46] D. M. Jacobs, G. D. Starkman and B. W. Lynn, Mon. Not. Roy. Astron. Soc. **450**, no. 4, 3418 (2015) [arXiv:1410.2236 [astro-ph.CO]].
- [47] J. A. Klimchuk, Solar Phys. **234**, 41 (2006) [astro-ph/0511841].
- [48] J. A. Klimchuk, [astro-ph/1709.07320].
- [49] A. Pauluhn and S. K. Solanki, Astron. Astrophys. **462**, 311 (2007) [astro-ph/0612585].
- [50] I. G. Hannah, S. Christe, S. Krucker, G. J. Hurford, H. S. Hudson and R. P. Lin, Astrophys. J. **677**, 704 (2008) [arXiv:0712.2544 [astro-ph]].

- [51] S. Bingert and H. Peter, *Astron. Astrophys.* **550**, A30 (2013) [arXiv:1211.6417 [astro-ph.SR]].
- [52] Klimchuk, J. A., Cargill, P. J. 2001, *Astrophys. J.*, **553**, 440 (2001);  
 Terzo, S., Reale, F., Miceli, M., et al., *Astrophys. J.*, **736**, 111 (2011);  
 Bradshaw, S. J., Klimchuk, J. A., and Reep, J. W., *Astrophys. J.*, **758**, 53 (2012);  
 D. B. Jess , M. Mathioudakis , P. H. Keys, *Astrophys. J.*, **795**, 172, (2014).  
 A. S. Kirichenko and S. A. Bogachev, *Astrophys. J.*, **840**, 45, (2017);  
 Cecilia Mac Cormack et al, *Astrophys. J.*, **843**, 70, (2017).
- [53] K. Lawson and A. R. Zhitnitsky, *Phys. Lett. B* **757**, 376 (2016) [arXiv:1510.02092 [astro-ph.GA]].
- [54] K. Lawson and A. Zhitnitsky, *JCAP* **1702**, no. 02, 049 (2017) [arXiv:1611.05900 [astro-ph.CO]].
- [55] K. Lawson, *Phys. Rev. D* **83**, 103520 (2011).
- [56] K. Lawson, *Phys. Rev. D* **88**, 043519 (2013) [arXiv:1208.0042 [astro-ph.HE]].
- [57] D. P. Anderson, E. T. Herrin, V. L. Teplitz and I. M. Tibuleac, *Bull. Seismol. Soc. Am.* **93**, 2363 (2003) [astro-ph/0205089].
- [58] Arnab Rai Choudhury, *The Physics of Fluids and Plasmas. An Introduction for Astrophysicists*, Cambridge University Press, 1998
- [59] P. Salucci and N. Turini, Evidences for Collisional Dark Matter In Galaxies? [arXiv:1707.01059 [astro-ph.CO]]
- [60] S. Bertolucci, K.Zioutas, S. Hofmann, M. Maroudas, The Sun and its Planets as detectors for invisible matter, *Physics of the Dark Universe* (2017), doi.org/10.1016/j.dark.2017.06.001, [arXiv:1602.03666 [astro-ph.CO]]